ARTICLE

Tracking Twisted Intramolecular Charge Transfer and Isomerization Dynamics in 9-(2,2-Dicyanovinyl) Julolidine Using Femtosecond Stimulated Raman Spectroscopy

Zhengxin Wang, Jiaming Jiang, Yifan Huang*, Weimin Liu*

School of Physical Science and Technology, ShanghaiTech University, Shanghai 201210, China

(Dated: Received on March 23, 2022; Accepted on May 29, 2022)

Understanding the mechanism of how micro-environments affect molecular rotors helps the design and development of molecular sensors. Here, we utilized femtosecond stimulated Raman spectroscopy, helped by quantum chemical calculation, to study the structural dynamics of 9-(2,2-dicyanovinyl) julolidine in cyclohexane, THF, and DMSO solvents. The obtained hydrogen out-of-plane (HOOP) mode and symmetric/anti-symmetric stretching of two nitriles (C≡N) indicate the rotation of the C_7=C_8 double bond and C_4–C_7 single bond in the excited-state which provide two non-radiative decay channels to effectively quench the excited-state population on local excited (LE) state via isomerization and twisted intramolecular charge transfer (TICT). In nonpolar solvent, the excited molecule in the LE state radiatively relaxes to the ground state or performs rotation motions via isomerization and TICT to deactivate fluorescence in the LE state. In the polar solvent, the isomerization plays a role to quench the LE state population; simultaneously, an ultrafast intramolecular charge transfer (ICT) from LE state to emissive ICT state was followed by an TICT between ICT state and dark ICT′ state.

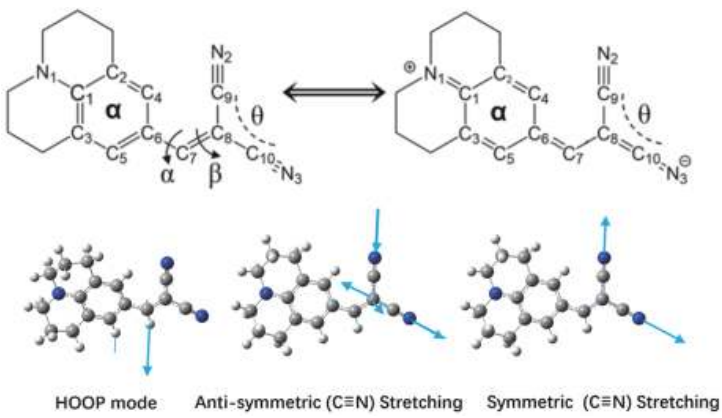

Key words: Femtosecond stimulated Raman spectroscopy, Twisted intralomecular charge transfer, Isomerization, Hydrogen out-of plane mode

I. INTRODUCTION

Several photochemical processes, such as charge transfer and photo-isomerization, can compete with the radiative decay of an excited state. This inspires researchers to develop sensitive fluorescent probes to display changes in the local environment [1]. The most interesting of this kind of fluorescent material are called molecular rotors [2–4]. The fluorescence quantum yield of this kind of molecule is influenced by variations in local temperature or viscosity since the internal rotation of a subunit contributes to the nonradiative decay of the excited state. However, the physical mechanism behind this effect is still in dispute, the fluorescence quenching is assigned to twisted intramolecular charge transfer (TICT) process through rotation around C–C single bond α (Scheme 1(a)) which leads to the formation of a nonradiative charge transfer state [5–10]. An

* Authors to whom correspondence should be addressed. E-mail: huangyf@shanghaitech.edu.cn, liuwm@shanghaitech.edu.cn

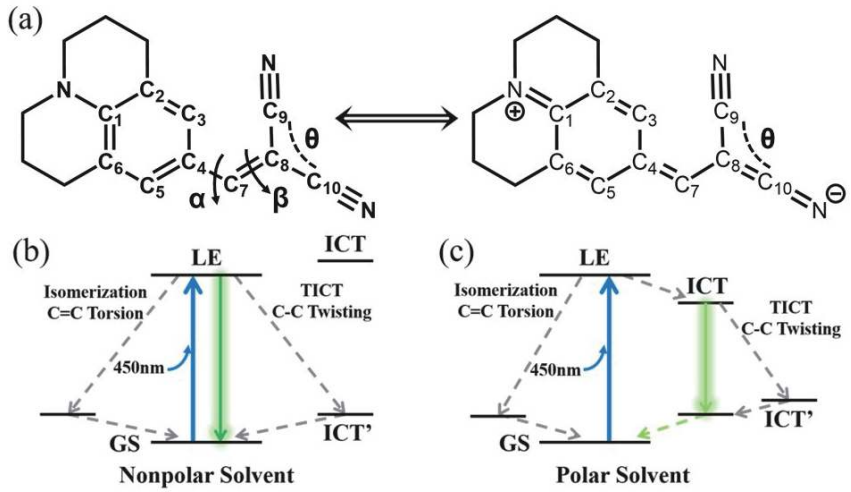

Scheme 1. (a) Natural and zwitterionic molecular structure of JDMN, (b) proposed model for JDMN in nonpolar solvent, and (c) proposed model for JDMN in polar solvent.

alternative view demonstrates that the mechanism includes internal conversion (IC) through isomerization of C=C double bond β (Scheme 1(a)) [11, 12]. While others acknowledged both of these happen simultaneously [13–15].

9-(2,2-Dicyanovinyl) julolidine (JDMN) is a prototypic molecular rotor with a zwitterionic character, which has been investigated broadly as a non-linear optical generator [16–18]. JDMN is a molecule of high polarity with a large electric dipole moment. Its value in the ground state (GS) is approximate 9.6 D and in the first excited-state is 18 D, respectively [19, 20]. Resonance Raman data and quantum mechanical calculations revealed that the GS and excited-states of JDMN contain a mixture of neutral and zwitterionic form [17, 18, 21].

Previously, the excited state dynamics of JDMN has been investigated using transient absorption, and time-resolved fluorescence spectroscopies [5, 11–15, 19]. In this research work, we used femtosecond stimulated Raman spectroscopy (FSRS), helped by quantum chemical calculation (density functional theory-DFT), to investigate the excited-state structural dynamics of JDMN. FSRS is a novel time-resolved vibrational technique with simultaneously high temporal and spectral (<15 cm^{-1}) resolution and has been successfully used to study the structural dynamics of molecules in photochemical and photobiological systems [22–26]. The experiment data of FSRS assisted by quantum calculations suggest that C_4–C_7 and C_7=C_8 bonds are rotated simultaneously in the excited state, and direct experimental evidence of zwitterionic character is observed.

II. FEMTOSECOND STIMULATED RAMAN SPECTROSCOPY (FSRS)

The fundamental laser pulses (Astrella, Coherent, Inc. 35 fs, 7 mJ pulse energy, 1 kHz) were split into three beams to generate a tunable narrowband picosecond (ps) Raman pump, a broadband femtosecond (fs) Raman probe, and an fs actinic pump. The actinic pump centered at 450 nm was generated by an optical parametric amplifier (OPA) (OPerA Solo, Coherent, Inc.) for excited-state FSRS. About 3 W of fundamental pulses was directed through a second harmonic bandwidth compressor (SHBC, Coherent, Inc.) to produce ps 400 nm pulses and then pump a ps-OPA system (TOPAS-400, Coherent, Inc.) to generate a ps pulse centered at 510 nm as the Raman pump. About 15 mW of the fundamental laser output was focused onto a 2-mm-thick single-crystal sapphire plate to obtain the supercontinuum white light as Raman probe. The instrument response time was measured to be ~150 fs.

The 9-(2,2-dicyanovinyl) julolidine was purchased from APExBIO Technology LLC. It was used without further purification.

III. RESULTS AND DISCUSSION

9-(2,2-Dicyanovinyl) julolidine (JDMN) consists of two moieties, julolidine and malononitrile, connected with C_4–C_7=C_8 bridge. In polar solvent, JDMN displays a zwitterion-like structure (Scheme 1(a)). That zwitterionic (charge separation) character increases with the increase of solvent polarity [27]. The steady-

DOI: 10.1063/1674-0068/cjcp2203046

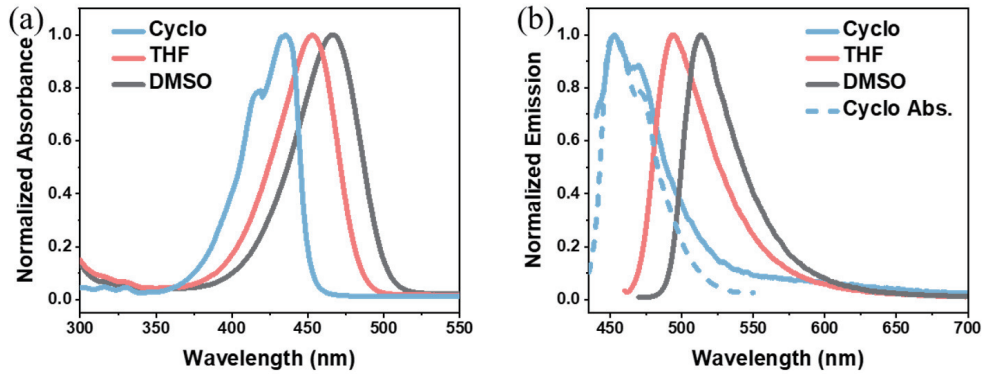

FIG. 1 (a) Steady-state absorption and (b) fluorescence spectra of JDMN in cyclohexane, THF, and DMSO; the blue dashed line (Cyclo Abs) in (b) is the mirror image of the absorption spectrum in cyclohexane.

state absorption and fluorescence spectra of JDMN in cyclohexane, THF, and DMSO are shown in FIG. 1. The absorption band shows a significant solvatochromic effect that the absorption peak redshifts from 440 nm in nonpolar cyclohexane to 466 nm in polar DMSO, the larger dielectric constant also corresponds to a larger stokes shift of fluorescence band indicating that this emissive excited-state is an intramolecular charge transfer (ICT) state in THF and DMSO [23, 28, 29]. In cyclohexane, the absorption and fluorescence bands of JDMN contain resolved vibronic structures with a sharp origin peak and a shoulder separated by ~1200 cm^{-1} in absorption and emission, resonance Raman studies of JDMN have attributed this shoulder to a composite of several vibrational modes of benzene and ethylene between 1000−1600 cm^{-1} [17], indicating that the excited-state is mainly located in the julolidine moiety of JDMN (local excited-state-LE state). Notably, as illustrated by the dashed lines in FIG. 1(b), the absorption and emission spectra in cyclohexane do not show mirror symmetry (bandwidth of emission spectrum is broader than that of absorption spectrum), which suggests possibly larger structural torsion in LE-S_1 state *versus* ground state-S_0 state [19]. As the dielectric constant increases, loss of vibronic structure in middle polar (THF) and polar (DMSO) solvents compared with nonpolar cyclohexane, the absorption spectrum becomes broader than that in nonpolar solvents indicating an inhomogeneous solvent broadening happened in polar solvents [19]. While the Franck-Condon activity in the emission spectra reductions with a growing solvent polarity leads to a narrowing of the emission bandwidth [30, 31], which can be reasonably interpreted as variable mixing of neutral and zwitterionic forms as a function of solvent polarity.

To get more experimental evidence of structural dynamics of JDMN, vibrational spectrum in a broad frequency domain with high time resolution is necessary. We applied the FSRS experiment of JDMN in three solvents upon the photoexcitation of the actinic pump centered at 450 nm. We strategically selected 510 nm Raman pump at the emission band of JDMN to pre-resonantly enhance FSRS signal, providing the excited-state Raman signals across the broad frequency range of 800–2400 cm^{-1}.

Since two rotation paths were identified for the JDMN chromophore in its excited state, a "conventional" isomerization (torsion) around the double bond $\beta(C_7{=}C_8)$ and an unusual twist around the adjacent (C_4–C_7) single bond α (see Scheme 1(a)) [13]. Notably, the C=C double bond torsional motions are shown to couple to a new coordinate of hydrogen out-of-plane (HOOP) mode whose role in the isomerization was identified theoretically and experimentally [32–34]. The implication of HOOP in the chromophore's isomerization has been confirmed by using FSRS in serval biological and chemical systems [22, 35, 36]. Here, the FSRS spectra of JDMN from 850 cm^{-1} to 1100 cm^{-1} are presented in FIG. 2. Aided by density functional theory (DFT-PBE1PBE) calculations, we identify a HOOP motion of C_7–H with a prominent intensity increase at ~940 cm^{-1} in cyclohexane (see FIG. 2(a) and FIG. 3(a)). The steady absorption and fluorescence spectra of JDMN in cyclohexane indicate that the excited state is mainly located in the julolidine part, reflecting a LE state dynamics upon photoexcitation. As shown in FIG. 2(b), the observed HOOP mode in cyclohexane displays single exponential decay with a time constant of ~995 fs, indicating the $C_7{=}C_8$ double bond isomerization on the LE state and the part of excited-state popu-

DOI: 10.1063/1674-0068/cjcp2203046

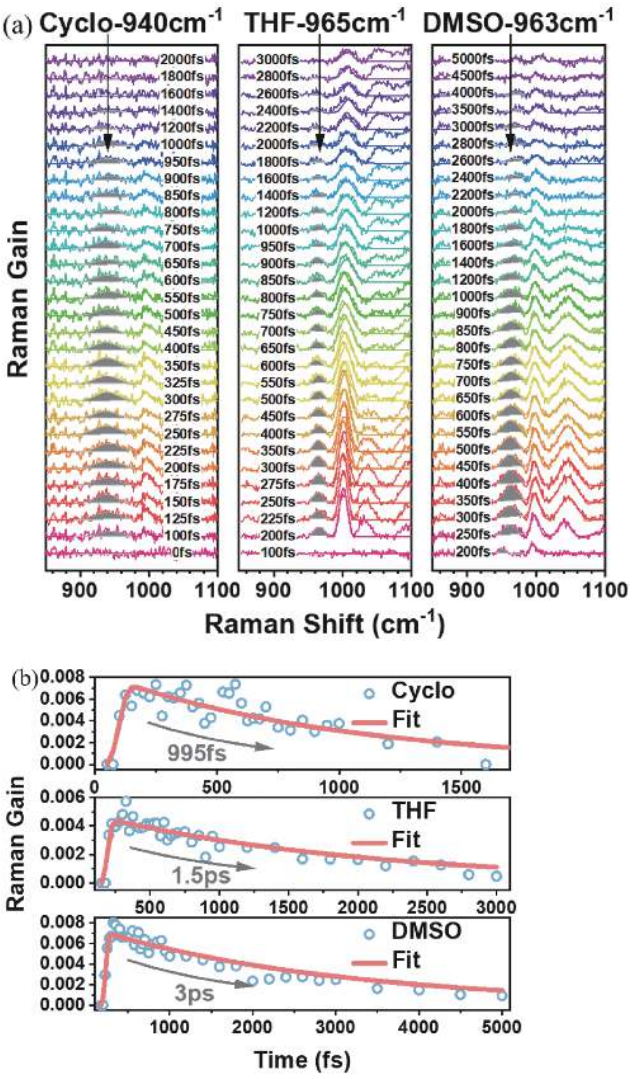

FIG. 2 (a) FSRS spectra of JDMN in cyclohexane, THF, and DMSO under 1100 cm^{-1}. (b) Transient Raman amplitudes of the HOOP mode in three solvents.

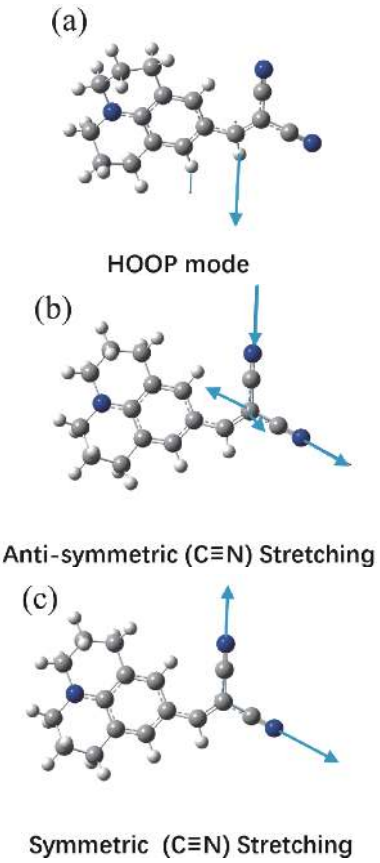

FIG. 3 DFT calculation showing the optimized structure of (a) HOOP mode, (b) anti-symmetric (C≡N) stretching mode, and (c) symmetric (C≡N) stretching mode.

lations on LE state go back to a dark hot GS directly via a conical intersection (CI). As the polarity increases, the dynamics of the HOOP mode exhibits a single exponential decay process of $\tau \approx 1.5$ ps in THF, and $\tau \approx 3$ ps in DMSO (see FIG. 2(b)). It shows that the viscosity of the solvents (cyclohexane: η=0.89 mPa·s, THF: $\eta = 0.46$ mPa·s, DMSO: $\eta = 2.0$ mPa·s) weakly affects the lifetime of HOOP mode of the excited JDMN which might be due to that the rotor (malononitrile moiety) is relatively small and can pack into cavities in the solvent structure [37]. Notably, the lifetime of C_7=C_8 rotation increases as the dielectric constant increases (cyclohexane: ε=2.02, THF: ε=7.58, DMSO: ε=46.68) which is consistent with the previous reports [13, 19]. Given that the energy gap at CI may affect the torsion lifetime around C_7=C_8, the energy gap in the solvent with a lower dielectric constant is smaller than that with a higher dielectric constant [13]. Consistent with the energy gap law, the IC rate in DMSO should be slower and therefore affect the rotational relaxations of the excited JDMN [13].

Notably, at delay time t=0 fs, the HOOP modes in THF and DMSO are blue-shifted by ~25 cm^{-1} and ~23 cm^{-1} relative to that in cyclohexane (FIG. 2(a)), which indicates a significant enhanced zwitterionic character in the excited-state as JDMN is dissolved in the medium (THF) and high (DMSO)-polar solvents. Quantum chemical calculations demonstrated that, in the GS, a more zwitterion-like structure is observed as solvent polarity increases, which indicates alternate positive and negative variations of the lengths of the double bond and the single bond along the whole JDMN molecule from the amino to the cyano nitrogen contributing to a bond length alternation (BLA) [27]. In the excited-state, the ~10 D change in dipole moment between the excited-state (18 D) and GS (9.6 D) states of JDMN reflects greatly increased zwitterionic (charge-separated) character in the LE-S_1 state which further

DOI: 10.1063/1674-0068/cjcp2203046

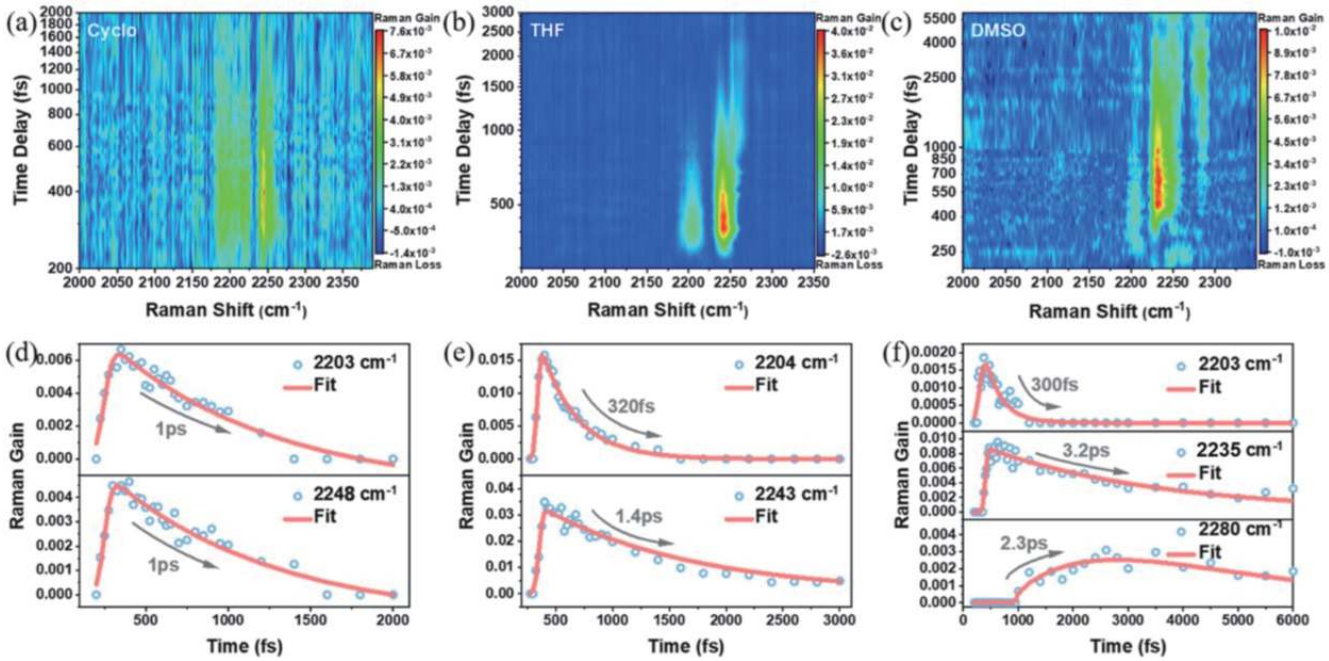

FIG. 4 Two-dimensional plot of the FSRS spectra of JDMN in (a) cyclohexane, (b) THF, and (c) DMSO above 2000 cm^{-1}. Transient Raman amplitudes of vibrational modes in (d) cyclohexane, (e) THF, and (f) DMSO.

varies the BLA value [12, 19, 27], the variation of the conjugated bond lengths thus leads to the significant blue shift of the HOOP mode in the excited-state.

The dynamics of HOOP mode suggests photoinduced isomerization via C_7=C_8 double bond rotation; however, whether the single bond twisting influences the photodynamics of JDMN remains unclear. To answer this question, the excited-state Raman signals in the range of 2000−2400 cm^{-1} are monitored. In this region, the C≡N group stretching modes of malononitrile moiety are dominant. C≡N group is usually a strong electron-withdrawing group and is present at one terminal end in most of the push-pull molecules [38, 39]. Given that the C≡N stretching mode has a large Raman cross-section in the frequency range of ~2200 cm^{-1} and is particularly convenient as it is a highly localized vibration with a frequency well separated from those of the other modes. Special attention has been paid to these stretching modes in FSRS measurement to investigate symmetry-breaking charge transfer dynamics [24, 40].

The FSRS spectra of JDMN above 2000 cm^{-1} are presented in FIG. 4. In the nonpolar cyclohexane, the FSRS spectra of JDMN exhibit two Raman modes at 2203 and 2248 cm^{-1} which are assigned to anti-symmetric and symmetric of the two C≡N bonds stretching modes in malononitrile moiety (see FIG. 3 (b) and (c)), both modes reveal a similar single exponential decay with a lifetime of 1 ps, as shown in FIG. 4 (a) and (d). In THF, the two vibrational modes shift to 2204 and 2243 cm^{-1} and exhibit distinct single exponential decay dynamics, the anti-symmetric C≡N stretching mode at 2203 cm^{-1} has an ultrafast decay lifetime of 320 fs, while the symmetric C≡N stretching mode undergoes 1.4 ps decay dynamics (see FIG. 4 (b) and (e)). In the highest polar DMSO, in addition to the two modes at 2203 and 2235 cm^{-1} with decay time constants of 300 fs and 3.2 ps, a third vibrational band at 2280 cm^{-1} emergs with a fast rise dynamic of 2.3 ps following a long lifetime exponential decay (see FIG. 4 (c) and (f)). It has been demonstrated that the rise of the symmetric C≡N stretching dynamics in the excited-state indicates an increase in the displacement contribution between C_{10} and C_6 atoms [41], which can be achieved through rotating the malononitrile moiety to change the distance between these two atoms (see Scheme 1(a)). Importantly, the dynamics of C≡N symmetric stretching modes in the three solvents exhibit the same decay lifetime as that obtained from the HOOP modes, which indicates that the malononitrile moiety rotates mainly via C_7=C_8 double bond torsion leading to quenching of excited-state through CI between the LE state and GS state. For the anti-symmetric C≡N stretching mode, the presence of this Raman mode in the excited-state results

DOI: 10.1063/1674-0068/cjcp2203046

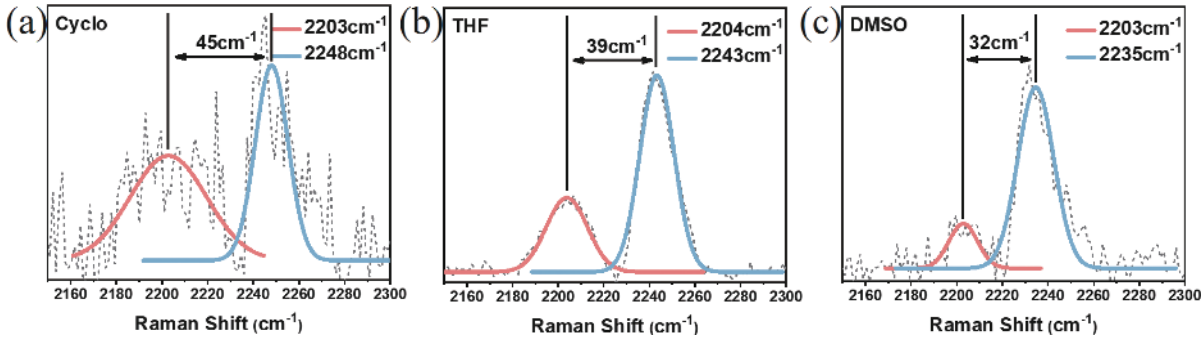

FIG. 5 The difference in peak frequency between the symmetric and the anti-symmetric stretching modes in (a) cyclohexane (45 cm^{-1}), (b) THF (39 cm^{-1}), and (c) DMSO (32 cm^{-1}) at delayed time zero of FSRS spectra.

from the changes in the coupling between the two nitriles (C_9≡N and C_{10}≡N) [41], which is closely related to local charge mobility in malononitrile moiety. The previous calculations have demonstrated that rotating around the C_4–C_7 single bond (TICT) leads to the formation of a metastable ICT state, and the barrier of TICT pathway is calculated to be lower than that of the double bond torsion, indicating that the TICT is faster than the double bond torsion [13]. Furthermore, the increase of polarity lowers the TICT energy barrier which makes the twisted ICT state easier to reach [29]. In our experiment, in middle polarity THF, the dynamics of anti-symmetric stretching Raman mode shows the 320 fs decay lifetime which can be attributed to that, after an ultrafast (less than 100 fs) ICT process [13] (LE-state to ICT state), the population on radiative ICT state decays to nonradiative ICT′ state via TICT process. Given that the JDMN molecule shows the zwitterionic character in polar solvents, the increased zwitterionic character upon photoexcitation indicates the change of dipole moment and highlights the further charge-shift nature via TICT. The decay dynamics of the anti-symmetric mode reveals a decoupling of the nitrile group due to charge redistribution in the malononitrile moiety. As the solvent polarity increases, the lifetime of this mode decreases a little bit to 300 fs in DMSO solvent, the TICT process eventually breaks the anti-symmetric stretching character, and the subsequent appearance of mode at 2280 cm^{-1} is assigned to the single nitrile stretching vibration mode [42], which provides a further valuable clue about the formation of charge separation in excited-state. Notably, in nonpolar cyclohexane, the anti-symmetric stretching mode is obtained, indicating possible TICT dynamics from LE state to the dark ICT state. Furthermore, as shown in FIG. 5, at time zero, the peak frequency difference between the symmetric and the antisymmetric stretching modes is ~45 cm^{-1} in cyclohexane; with the solvent polarity increasing, the difference decreases to ~39 cm^{-1} in THF and to ~32 cm^{-1} in DMSO; which indicates that the angle (θ) between two nitriles (see Scheme 1(a)) increases as the solvent polarity increases [43].

IV. CONCLUSION

In this study, we apply the FSRS experiments aided by DFT calculations to demonstrate the excited-state structural dynamics of JDMN in nonpolar and polar solvents. The observation of spectator Raman C_7–H HOOP mode and symmetric/anti-symmetric stretching of two nitriles (C_9≡N and C_{10}≡N) indicate the rotation of the C_7=C_8 double bond and C_4–C_7 single bond in the excited-state which provide parallel non-radiative decay channels to effectively quench the LE state population via isomerization and TICT. Triggered by double bond isomerization and TICT processes, the overall kinetic traces of JDMN in nonpolar and polar solvents can thus be depicted in Scheme 1 (b) and (c). The two proposed fluorescence deactivation pathways are present in JDMN in cyclohexane after photoexcitation from the GS and the excited molecule in the LE state can radiatively relax to the GS or perform rotation motions around either the C_4–C_7 single bond or C_7=C_8 double bond (see Scheme 1(a)). Both rotations result in fluorescence deactivation. The rotation around the C_4–C_7 single bond yields a TICT transition from LE to a dark ICT state; rotation around C_7=C_8 double bond leads to isomerization and instantaneous nonradiative relaxation. In the polar solvent, the isomerization through C_7=C_8 double bond plays a role in quenching the LE state population to GS; simultaneously, intramolecular charge transfer from LE state to ICT state with a time constant of ~100 fs was obtained [13] which

DOI: 10.1063/1674-0068/cjcp2203046

follow by an ultrafast TICT process from ICT state to dark ICT′ state in 320 fs in THF and 300 fs in DMSO.

V. ACKNOWLEDGMENTS

This work was supported by the Natural Science Foundation of Shanghai (20ZR1436300), the National Natural Science Foundation of China (No.21872094).

[1] T. D. James and S. Shinkai, in *Host-Guest Chemistry: Mimetic Approaches to Study Carbohydrate Recognition*, S. Penadés Ed., Berlin, Heidelberg: Springer Berlin Heidelberg, 159 (2002).
[2] M. A. Haidekker, T. Ling, M. Anglo, H. Y. Stevens, J. A. Frangos, and E. A. Theodorakis, Chem. Biol. **8**, 123 (2001).
[3] T. Iio, M. Itakura, S. Takahashi, and S. Sawada, J. Biol. Chem. **109**, 499 (1991).
[4] P. Gautam and A. Harriman, J. Chem. Soc. Faraday Trans. **90**, 697 (1994).
[5] Z. A. Dreger, J. O. White, and H. G. Drickamer, Chem. Phys. Lett. **290**, 399 (1998).
[6] C. E. Kung and J. K. Reed, Biochemistry-Us **28**, 6678 (1989).
[7] T. Iwaki, C. Torigoe, M. Noji, and M. Nakanishi, Biochemistry-Us **32**, 7589 (1993).
[8] M. A. Haidekker and E. A. Theodorakis, Org. Biomol. Chem. **5**, 1669 (2007).
[9] K. I. Gutkowski, M. L. Japas, and P. F. Aramendía, Chem. Phys. Lett. **426**, 329 (2006).
[10] A. Paul and A. Samanta, J. Phys. Chem. **B 112**, 16626 (2008).
[11] A. Safarzadeh-Amiri, Chem. Phys. Lett. **129**, 225 (1986).
[12] A. Y. Jee, E. Bae, and M. Lee, J. Phys. Chem. **B 113**, 16508 (2009).
[13] S. Q. Yang and K. L. Han, J. Phys. Chem. **A 120**, 4961 (2016).
[14] M. S. A. Abdel-Mottaleb, R. O. Loutfy, and R. Lapouyade, J. Photochem. Photobiol. **A 48**, 87 (1989).
[15] S. Mqadmi and A. Pollet, J. Photochem. Photobiol. A **53**, 275 (1990).
[16] M. Blanchard-Desce, R. Wortmann, S. Lebus, J. M. Lehn, and P. Krämer, Chem. Phys. Lett. **243**, 526 (1995).
[17] A. M. Moran, D. S. Egolf, M. Blanchard-Desce, and A. M. Kelley, J. Chem. Phys. **116**, 2542 (2002).
[18] A. M. Moran, A. M. Kelley, and S. Tretiak, Chem. Phys. Lett. **367**, 293 (2003).
[19] H. Jin, M. Liang, S. Arzhantsev, X. Li, and M. Maroncelli, J. Phys. Chem **B 114**, 7565 (2010).
[20] R. O. Loutfy, Pure Appl. Chem. **58**, 1239 (1986).
[21] J. Guthmuller and B. Champagne, J. Chem. Phys. **127**, 164507 (2007).
[22] J. Wei, Y. Wu, R. Pu, L. Shi, J. Jiang, J. Du, Z. Guo, Y. Huang, and W. Liu, J. Phys. Chem. Lett. **12**, 4466 (2021).
[23] W. Xu, L. Wei, Z. Wang, R. Zhu, J. Jiang, H. Liu, J. Du, T. C. Weng, Y. B. Zhang, Y. Huang, and W. Liu, J. Phys. Chem. **B 125**, 10796 (2021).
[24] W. Zhang, W. Xu, G. Zhang, J. Kong, X. Niu, J. M. W. Chan, W. Liu, and A. Xia, J. Phys. Chem. **B 125**, 4456 (2021).
[25] W. Liu, L. Tang, B. G. Oscar, Y. Wang, C. Chen, and C. Fang, J. Phys. Chem. Lett. **8**, 997 (2017).
[26] W. Liu, Y. Wang, L. Tang, B. G. Oscar, L. Zhu, and C. Fang, Chem. Sci. **7**, 5484 (2016).
[27] B. Mennucci, C. Cappelli, R. Cammi, and J. Tomasi, Theor. Chem. Acc. **117**, 1029 (2007).
[28] T. Subina, S. Amirjalayer, B. Mennucci, S. Woutersen, M. Hilbers, D. Bonn, and A. M. Brouwer, J. Phys. Chem. Lett. **7**, 4285 (2016).
[29] G. Duvanel, J. Grilj, H. Chaumeil, P. Jacques, and E. Vauthey, Photochem. Photobiol. Sci. **9**, 908 (2010).
[30] B. Boldrini, E. Cavalli, A. Painelli, and F. Terenziani, J. Phys. Chem. **A 106**, 6286 (2002).
[31] S. Arzhantsev, K. A. Zachariasse, and M. Maroncelli, J. Phys. Chem. A **110**, 3454 (2006).
[32] O. Weingart, Chem. Phys. **349**, 348 (2008).
[33] E. V. Gromov, J. Chem. Phys. **141**, 224308 (2014).
[34] E. V. Gromov, I. Burghardt, H. Köppel, and L. S. Cederbaum, J. Phys. Chem. **A 115**, 9237 (2011).
[35] P. Kukura, D. W. McCamant, S. Yoon, D. B. Wandschneider, and R. A. Mathies, Science **310**, 1006 (2005).
[36] J. Dasgupta, R. R. Frontiera, K. C. Taylor, J. C. Lagarias, and R. A. Mathies, Proc. Natl. Acad. Sci. USA **106**, 1784 (2009).
[37] B. D. Allen, A. C. Benniston, A. Harriman, S. A. Rostron, and C. F. Yu, Phys. Chem. Chem. Phys. **7**, 3035 (2005).
[38] Y. Zhang, L. Yuan, S. Jia, X. Liu, J. Zhao, and G. Yin, Phys. Chem. Chem. Phys. **21**, 3218 (2019).
[39] J. Mei, J. Z. Sun, A. Qin, and B. Z. Tang, Dyes Pigm. **141**, 366 (2017).
[40] W. Zhang, J. Kong, W. Xu, X. Niu, D. Song, W. Liu, and A. Xia, Chin. J. Chem. Phys. **35**, 69 (2022).
[41] O. Louant, B. Champagne, and V. Liegeois, Chem. Phys. Lett. **634**, 249 (2015).
[42] Y. N. Mabkhot, S. S. Al-Showiman, A. Barakat, S. M. Soliman, N. A. Kheder, M. M. Alharbi, A. Asayari, A. B. Muhsinah, A. Ullah, and S. L. Badshah, BMC Chemistry **13**, 25 (2019).
[43] Monika, S. Inaoka, K. Iwata, and S. Saha, Spectrochim. Acta A Mol. Biomol. Spectrosc. **224**, 117419 (2020).

DOI: 10.1063/1674-0068/cjcp2203046